

## High Performance Tokamak Experiments with Ferritic Steel Wall on JFT-2M

K. Tsuzuki 1), H. Kimura 1), H. Kawashima 1), M. Sato 1), K. Kamiya 1), K. Shinohara 1), H. Ogawa, K. Hoshino 1), M. Bakhtiar 1), S. Kasai 1), K. Uehara 1), H. Sasao 1), Y. Kusama 1), N. Isei 1), Y. Miura 1), T. Ogawa 1), M. Yamamoto 1), T. Shibata 1), K. Kikuchi 1), K. Miyachi 1), T. Ito 2), H. Ajikawa 2), S. Nomura 2), H. Tsutsui 2), R. Shimada 2), T. Ido 3), Y. Hamada 3), N. Fukumoto 4), M. Nagata 4), T. Uyama 4), H. Niimi 5), S. Yatsu 5), N. Kayukawa 5), T. Hino 5), Y. Hirohata 5), Y. Nagashima, 6), A. Ejiri 6), A. Amemiya 7), Y. Sadamoto 8), A. Tsushima 9)

1)Naka Fusion Research Establishment, Japan Atomic Energy Research Institute

2)Tokyo Institute of Technology, 3)National Institute for Fusion Science,

4)Himeji Institute of Technology, 5)Hokkaido University, 6) University of Tokyo,

7) The Institute of Physical and Chemical Research, 8)Joetsu University of education,

9)Yokohama National University

E-mail: tsuzukik@fusion.naka.jaeri.go.jp

**Abstract.** In the JFT-2M tokamak compatibility between plasma and the low activation ferritic steel, which is candidate material of a fusion reactor, has been investigated step by step. We have entered the 3rd stage of Advanced Material Tokamak EXperiment (AMTEX), where the inside of vacuum vessel wall is fully covered with ferritic steel plates (Ferritic Inside Wall; FIW). The effects of FIW have been investigated on the plasma production, the impurity release, the operation region, and H-mode characteristics. No deteriorative effect has been observed up to now. High normalized beta plasma of  $\beta_N \sim 3$  having both internal transport barrier and the steady H-mode edge was obtained. Remarkable reduction of ripple trapped loss from  $0.26 \text{ MW/m}^2$  (w/o ferritic steel) to less than  $0.01 \text{ MW/m}^2$  was demonstrated due to optimization of the thickness profile of FIW. The effect of the localized ripple was also investigated with additional ferritic plates outside the vacuum vessel. In parallel with AMTEX, advanced and basic research for the development of high performance plasma such as evaluation of fluctuation induced particle flux and development of advanced fuelling (compact toroid injection) are also performed on JFT-2M.

### 1. Introduction

A low activation ferritic steel (such as F82H [1]) is a leading candidate material for a fusion demonstration reactor [2] because of its better properties for heat and neutron load, compared to austenite stainless steel. In addition, application of ferromagnetic material is planned in ITER aiming at reducing toroidal field ripple [3-5]. However, the effect of ferromagnetism on plasma control, stability and confinement is not well understood. Vacuum properties could also be problems because it easily rusts in the air [6]. Thus compatibility with plasma, in view of ferromagnetic effects and vacuum properties should be investigated. In small tokamak, HT-2, the ferritic steel, F82H, was installed inside the vacuum vessel. The compatibility of the ferritic steel was well demonstrated for ohmic heating plasma [7]. To investigate the compatibility with higher performance plasma, the Advanced Material Tokamak EXperiment (AMTEX) program is being performed, in the medium size tokamak JFT-2M ( $R=1.31 \text{ m}$ ,  $a \leq 0.35 \text{ m}$ ,  $k \leq 1.7$ ,  $B_{t0} \leq 2.2 \text{ T}$ ) [5,8-11]. In the last IAEA Fusion Energy Conference, results of the 1<sup>st</sup> stage of AMTEX were presented, where ferritic plates (FPs) were installed between the vacuum vessel and toroidal field coils, aiming at reducing the toroidal field ripple (similar configuration as ITER) [8,9]. In the second stage, the FPs of thickness 7 mm were installed along the whole toroidal circumference in the low field side above and below the horizontal ports. They covered  $\sim 20\%$  of the inside area of the vacuum vessel. No adverse effects of ferritic steel on the plasma operation and stability was observed at least for the normalized beta up to 2.7 [9-11]. With these encouraging results, we have entered the 3<sup>rd</sup> stage of AMTEX. The main purpose of this stage is 1) an investigation of the compatibility between plasma and a full covering ferritic inside wall (FIW) as a simulation of

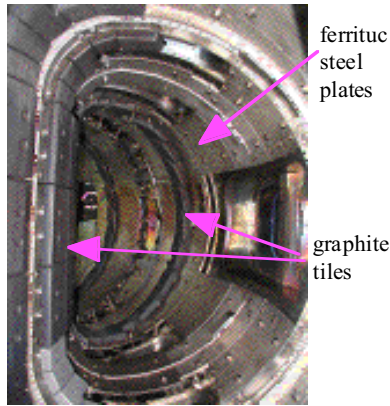


Fig.1 Picture of inside vacuum vessel after installation of FIW, magnetic sensors and graphite tiles.

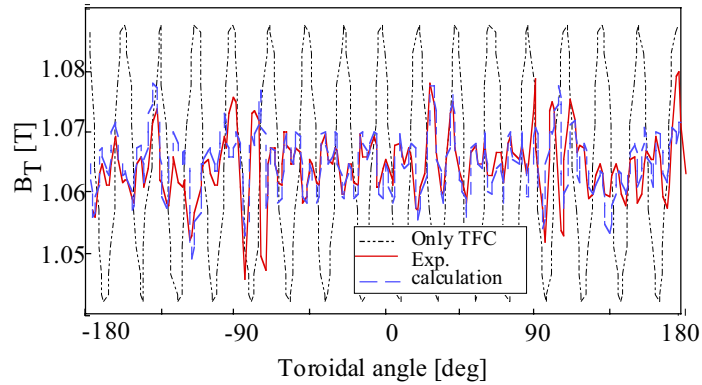


Fig. 2. Toroidal field ripple distribution.

blanket wall of the demo-reactor and 2) a demonstration of the significant reduction of the toroidal field ripple by optimizing the thickness profile of FIW. The setup and results are presented from Section 2 to Section 6.

In parallel with the AMTEX program, advanced and basic research for development of the high performance tokamak plasma are also performed with an MSE polarimetry, a heavy ion beam probe and a compact toroid injector etc. These results are shown from Section 7 to Section 9.

## 2. Design and Installation of Ferritic Steel

The ferritic inside wall (FIW) was installed along the vacuum vessel, keeping a distance of 30 mm from the inside surface of the vacuum vessel, so that the similar plasma configuration and shape as before can be obtained. The thickness of the ferritic steel is determined to meet both magnetic effect and ripple reduction. When the frequency of magnetic fluctuation increases, the effect of the eddy current increases, and thus, the effect of ferromagnetism are weakened [10]. The average thickness is determined to be 8 mm so that the effect of eddy current exceeds the ferromagnetic effect for typical frequency of tearing mode on JFT-2M (>6kHz). Furthermore, reduction of toroidal field ripple for almost 1/4 as large as that without FIW was conducted by optimization of thickness profile (6mm, 8mm, and 10.5mm) of FIW. Most of the magnetic sensors were installed on plasma side of the ferritic steel. Part of them were installed behind FIW to investigate shielding effect of the ferritic steel. Graphite tiles were installed on FIW keeping a distance of 50 mm. The configuration is similar to the previous one, namely, the high-field side was fully covered with the graphite tiles and the divertor region and low field side were covered discretely with them. Thus, main plasma-facing component is the graphite tiles and FIW is exposed to peripheral plasma.

Precise 3-D magnetic field measurements inside the vacuum vessel were carried out with rails, a vehicle, and hole elements installed inside the vacuum vessel. The magnetic field was measured for whole toroidal angle (192 points in toroidal direction and 5 points in poloidal direction, 3-Dcomponent (X, Y, Z) for each points). The results are shown in Fig.2. The experimental results are close to the calculated one. The designed value of the toroidal field ripple has been realized. It should be noted that the toroidal periodicity of the magnetic field is broken due to the limitation of installation area of the FIW by interferences with the existing component such as neutral beam ports. The measurement also indicated that a shift of the central axis of the vacuum vessel from that of the toroidal field coils is  $\sim 3$  mm. Since the FIW was installed along the vacuum vessel, the shift of the vacuum vessel induces low-n error field, which might induce locked mode [12]. However, in the case of  $m/n=2/1$  component ( $B_{r21}$ ), which is regarded as the most dangerous mode for locked mode, induced

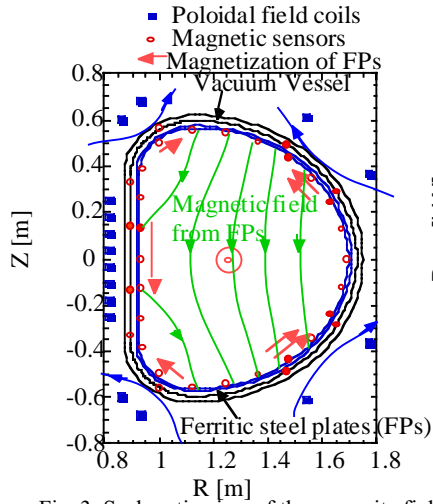


Fig. 3. Schematic view of the magnetic field caused by the ferritic steel.

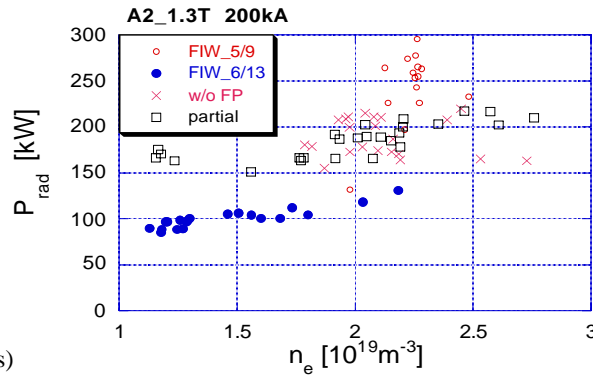


Fig. 4 Total radiation loss against line averaged density for limiter discharges of  $I_p=200\text{kA}$  and  $B_T=1.3\text{ T}$ . The loss is larger at initial phase (FIW 5/9) but smaller after experiments for  $\sim 1$  month (FIW 6/13).

error field due to the shift of  $\sim 3\text{ mm}$  is less than  $(B_{r21}/B_t=4\times 10^{-5})$ . This is much lower than the allowable limit for a joule heating plasma ( $B_{r21}/B_t=2\times 10^{-4}$ ) [12,13].

### 3. Wall Conditioning

The same procedure as the second stage was applied on the FPs, namely (1) removal of oxide layer by machining, (2) degreasing, and (3)  $350^\circ\text{C}$  baking for 20 hours [14]. Impurity release was not problem in the second stage [10]. However, it took 6 months for the installation (10days for the 2nd stage), and thus, the oxidation during air exposure might degrade the vacuum properties. The vacuum properties of the ferritic steel, which had been exposed to air for 2 months and slightly oxidized, were investigated in a test-stand, prior to the tokamak experiment. It has been confirmed that the out gas rate from the ferritic steel is sufficiently low for the FIW ( $10^{-8}\text{ Pam}^3/\text{sm}^2$ ) [15].

The usual procedure was applied in the initial pumping just after the installation of the FIW, namely, baking at  $120^\circ\text{C}$  for 3weeks and Taylor discharge cleaning (TDC) for 30 hours. The obtained base pressure was  $6\times 10^{-6}\text{ Pa}$ , which is same as that before the installation of FIW, as is predicted from the test-stand experiment. As for a discharge cleaning, the Taylor discharge cleaning was performed without changing discharge conditions, namely, working gas:  $\text{H}_2$ , pulse length:  $\sim 10\text{ ms}$ , interval:  $0.7\text{ sec}$ , pressure:  $2\times 10^{-4}\text{ Pa}$ . The partial pressure of  $\text{H}_2\text{O}$ ,  $\text{CO}$  and  $\text{CO}_2$  clearly increased when the TDC ignited and the out gas rate is 1.5 times as large as the case without ferritic wall. It means that the TDC is effective to remove oxygen impurity though the ferritic wall affects the magnetic structure. The glow discharge was also ignited and utilized to reduce hydrogen recycling.

### 4. Plasma Production and Impurity Release

To evaluate the effects of FIW on the plasma control, the magnetic field caused by the FIW was calculated with the equilibrium code including the effect of ferritic steel. Figure 3 shows schematic cross-sectional view of the magnetic field. The FPs are magnetized in the direction of poloidal field (typically, specific magnetization is  $2 \sim 3$ ). In a case of the elongated plasma, direction of the magnetization of ferritic steel is opposite in diverter region. Thus stray field forms vertical field as shown in the figure. It weakens the vertical field by  $\sim 10\%$ . In addition, this field affects magnetic sensors located on FIW. The JFT-2M uses 24 magnetic probes and 8 flux loops for plasma control and equilibrium calculation. The magnetic field caused by FIW is in the order of several percentage of the averaged poloidal

field at the probe position. If the separatrix (or last closed flux surface) is estimated without considering the effect on the magnetic sensors, major radius of the separatrix is  $\sim 1$  cm smaller than the real one. The vertical field from FIW can be compensated by increasing vertical field by  $\sim 10\%$ . The shift of plasma position can also be compensated by changing the setting value of the plasma control system.

As is predicted from the calculation, tokamak discharges were obtained without a marked change in the plasma control system. Increase in vertical field by  $\sim 10\%$  compared to the value w/o FIW was observed, which is consistent with calculated results.

As a measure of impurity release during the discharge, total radiation loss is shown in Fig. 4 for limiter discharges at  $B_T=1.3$  T and  $I_p=200$  kA. The total radiation loss for initial 1 month was slightly higher than the cases without FPs and partial coverage. After experiments of 1 month, it was decreased by  $\sim 20\%$  of the previous level. The oxygen line intensity measured by the visible spectroscopy became almost half of the previous level. The metal impurity measured by a vacuum ultraviolet spectroscopy was under the detection level. Thus, it is concluded that impurity release from the ferritic steel is not large in this experimental condition (main plasma facing component is graphite tiles), and improvement of the oxygen level could be attributed by the replacement of the graphite tiles.

After a series of experiment, boron coating was carried to obtain higher performance plasma by reducing impurities in the plasma. The experiments related to plasma stability and confinement were mainly carried out after the boron coating.

## 5. Investigation of Ripple Loss [16]

The ripple loss was evaluated with an infrared TV system (IRTV). Fast hydrogen ions are supplied by neutral beam injection (NBI) with its primary energy of 36 keV (CO-direction on  $I_p$ , tangentially on  $B_T$ ). The injection power is about 500 kW. The maximum heat flux due to the ripple trapped loss decreased from  $0.26$  MW/m<sup>2</sup> (w/o ferritic steel) to less than  $0.01$  MW/m<sup>2</sup> (with FIW) in optimized case ( $B_T \sim 1.3$ T).

As indicated in Fig.2, the toroidal field ripple is not reduced uniformly because of the limited installation of FIW. Such situation might also occur in a demo-reactor. In addition, large local ripple could be used for low energy beam injection and He exhaust [17-19]. Thus, understanding of the behavior of fast ions with complex ripple, including the large local ripple, is important. To investigate these effects experimentally, the ferritic steel plates outside the vacuum vessel were used to induce strongly localized ripple. The results show that the ripple loss depends on ripple well structure, e.g. the thickness of the ripple well. In other words, whole structure of the magnetic field has to be considered to analyze the ripple loss behavior. The experimental results were almost consistent with the newly developed Fully three Dimensional magnetic field Orbit-Following Monte-Carlo (F3D OFMC) code including the three dimensional complex structure of the toroidal field ripple and the non-axisymmetric first wall geometry. From the F3D OFMC calculation, the total loss of fast ions with FIW is about  $1/3$  as large as that with only TFC.

## 6. Effect of the Ferritic Steel on Plasma Performance

Figure 5 shows Hugill diagram after the FIW installation and boron coating. The density can be increased near Greenwald density and the safety factor,  $q$ , can be decreased around 2. It was reported that the region, where collapse due to a tearing mode occurs, exists around  $q \sim 3$ ,  $n_e \sim 1 \times 10^{19}$  m<sup>-3</sup> [11,20] as indicated in the figure. This region didn't change by the ferritic steel installation, which means that the effect of FIW on tearing mode is negligible. It should be noted that the ratio of minor radius of the resonance surface ( $r_s$ ) and the FIW ( $d$ ) is  $d/r_s \sim 1.6$ . The calculation code to clarify the wall effect is under development.

Growth rate of vertical instability was measured by switching off the feed-back control during the discharge [21]. The ferritic steel makes vertical instability unstable in qualitative

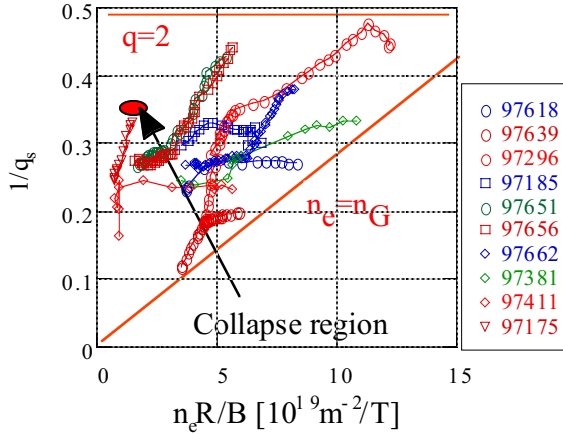


Fig.5 Hugill diagram with ferritic inside wall. The density can be increased near Greenwald density and the safety factor,  $q$ , can be decreased around 2.

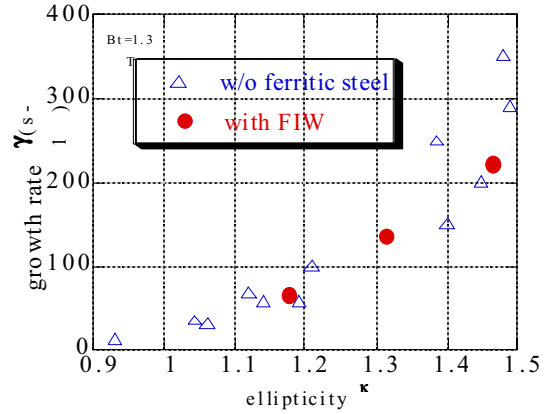


Fig.6 Growth rate of vertical instability against elongation. The growth rate didn't change by the installation of the FIW

manner, because the vertical shift of plasma causes unbalance of magnetization, which enhances the shift. However, this effect is limited within a few percentages. On the other hand, FIW acts as an additional conductive wall, which makes the instability stable. Experimental results shown in Fig. 6. The growth rate didn't change by the FIW installation presumably due to the compensation of above effects.

In the single-null divertor configuration, H-mode was obtained with similar conditions as before. The threshold power for the L-H transition is 420kW at  $B_T=1.3$  T,  $I_p=200$  kA, and  $n_e=3 \times 10^{19} \text{ m}^{-3}$ . It is almost the same as the value before the FIW installation (440 kW) and comparable to the value from scaling low  $\sim 500$  kW [22]. Averaged H factor ( $H_{89P}$ ) is  $\sim 1.8$  for ELMy H-mode, which is also comparable to the previous results.

Thus, no adverse effect of FIW on plasma confinement and stability has been observed up to now.

## 7. High Beta Experiment

In parallel with the AMTEX program, the advanced and basic studies for development of high performance plasma are performed on JFT-2M. As for the H-mode study, an attractive new operating regime, which is named "High Recycling Steady" (HRS) H-mode, have been

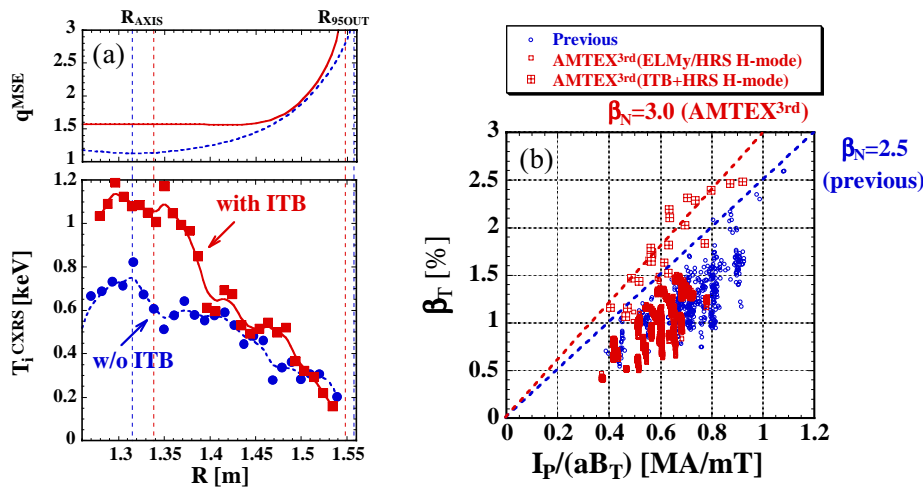


Fig.7 (a) profile of safety factor  $q$  and ion temperature, estimated from MSE and CXRS in the case with internal transport barrier, (b) toroidal beta against normalized current. The slope of the plot corresponds to normalized beta. In some condition.

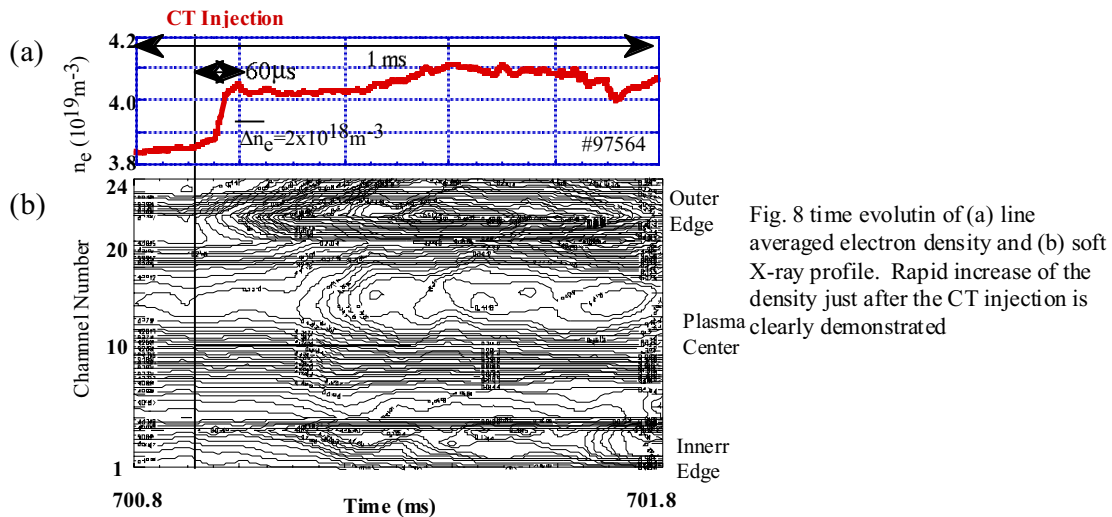


Fig. 8 time evolution of (a) line averaged electron density and (b) soft X-ray profile. Rapid increase of the density just after the CT injection is clearly demonstrated

discovered. It was first observed with deuterium saturated boronized wall. Important features of this mode are, (1) the steady-state H-mode edge condition at high density with good energy confinement, (2) the complete disappearance of giant ELMs, and (3) the compatibility with the internal transport barrier (ITB) [23]. The HRS was observed in high density region ( $n_e/n_{GW} > 0.4$ ), including the low safety factor region ( $2 < q_{95} \leq 3$ ). The formation of ITB was typically observed in low  $B_T$  ( $< 1.1T$ ) conditions during balance neutral beam injection of  $\sim 1.4$  MW (full power). The ion temperature measured by charge exchange recombination spectroscopy (CXRS) clearly peaked, which indicate the formation of ITB around  $r/a=0.1\sim 0.2$  as shown in Fig. 7a. The  $q$ -profile also changes from monotonic one to zero/weak shear in the plasma core region. To show the effect of the ITB formation on normalized beta, toroidal beta values are plotted against normalized current ( $I_p/aB_T$ ) in Fig. 7b. The slope of the figure corresponds to normalized beta ( $\beta_N$ ). In the cases without ITB, the normalized beta is limited less than 2.5. This value is same as previous results, without FIW and boronization. The  $\beta_N$  increased to 3.0 with the ITB as shown in box-plus in the Fig. 7b. This increase can be attributed to the improvement of the core confinement with keeping the steady H mode edge. The experiment was performed in the presence of FIW described above. These results are also import as the demonstration of compatibility of such FIW with high normalized beta plasma up to 3.0.

## 8. Estimation of Particle Flux in H-mode

The estimation of fluctuation induced particle flux at L-H transition is important for understanding of H-mode behavior. To investigate the flux, the fluctuations of the potential and the density were measured by Heavy Ion Beam Probe (HIBP) [24]. Poloidal wave number of the fluctuation was evaluated by taking several sample volumes located on almost the same magnetic flux surface at the same time. Using the measured wave number  $1\sim 2$   $\text{cm}^{-1}$  in L mode plasma, the radial particle flux induced by the fluctuation is evaluated. In the frequency range up to 100 kHz, it was found that the particle flux in L mode plasma is dominated in the frequency range of 20-60kHz. After the L-H transition, the flux of this frequency range almost disappeared. In H-mode phase, the Doppler-shifted fluctuation possibly exists in the frequency range of 100 kHz and more, but it couldn't measured mainly due to cross talk of the amplifier.

## 9. Advanced Fuelling (Compact Toroid Injection)

Compact toroid (CT) injection is an advanced method of the particle fueling into the plasma, and being investigated on JFT-2M. Prior to the injection experiment in 2002, the CT injector was modified in 2001, aiming at improving injection efficiency, i.e., a focus corn was replaced to straight type at the nozzle and the shape of the pre-compression region was modified to reduce focusing effect. In CT injection experiments into JFT-2M plasma, rapid increase of electron density within 60  $\mu\text{s}$  was clearly observed as shown in Fig. 8a. This is the first demonstration of the density increase in such a time scale. Figure 8b shows profile of soft X-ray. The intensity of weak field side initially increased and is kept for  $\sim 100 \mu\text{s}$ . Then it propagated to the plasma center. The fuelling efficiency within the rapid phase (60  $\mu\text{s}$ ) was estimated to be 25% by  $(\Delta n_e \times V_{\text{plasma}}) / (n_{\text{CT}} \times V_{\text{CT}})$ . In the case of other discharges, the time constant of the density increase is  $\sim 500 \mu\text{s}$ . This time scale is much shorter than that with only gas puff. The mechanism of density increase with different time scale has been unclear so far.

In addition, we have a plan to inject CTs vertically into the JFT-2M tokamak by using a curved drift tube for the improvement of CT injection efficiency. The proof-of-principle experiments on CT transport with a curved drift tube have been successfully carried out at the Himeji Institute of Technology [25].

## Summary

The compatibility of low activation ferritic steel with plasma has been investigated in the JFT-2M with respect to ferromagnetic effects and impurity release. The vacuum vessel was fully covered with the ferritic steel as a simulation of blanket wall (FIW: Ferritic Inside Wall). The base pressure with FIW was almost same as the cases without ferritic steel. Tokamak discharge was obtained without marked change in plasma control system as is consistent with the expectation. The radiation loss and oxygen line intensity decreased for 20% probably due to replacement of graphite tiles. The metal line intensity measured by a vacuum ultraviolet spectroscopy was under the detection level. As a measure of plasma stability and confinement, the operation region, threshold power for L-H transition and H factor were investigated, showing similar results as the case before the FIW installation. During the study, attractive operating regime named High Recycling Steady (HRS) H-mode, have been discovered. This mode has characteristics as follows; the steady-state H-mode edge condition at high density with good energy confinement, the complete disappearance of Giant ELMs, and the compatibility with internal transport barrier (ITB) [23]. The normalized beta ( $\beta_N$ ) increased up to  $\sim 3.0$ , which is the highest value of JFT-2M by the combination of steady H-mode edge and improvement of core confinement. This result is also important as a demonstration of compatibility of ferritic steel wall with high-normalized beta plasma.

As for the ripple loss, remarkable reduction from  $0.26 \text{ MW/m}^2$  (w/o ferritic steel) to less than  $0.01 \text{ MW/m}^2$  (with FIW) was demonstrated in optimized case ( $B_T \sim 1.3\text{T}$ ). To investigate the effect of complex field produced by the ferritic steel, the ferritic steel outside the vacuum vessel was additionally installed for inducing strongly localized ripple. The results show that the ripple loss depend on ripple well structure, e.g. the thickness of the ripple well. The experimental results were almost consistent with the newly developed Fully three Dimensional magnetic field Orbit-Following Monte-Carlo (F3D OFMC) code including the three dimensional complex structure of the toroidal field ripple and the non-axisymmetric first wall geometry.

As for the H-mode study, the fluctuation induced particle flux was evaluated with Heavy Ion Beam Probe (HIBP). A peak of the flux in L mode plasma is observed in the frequency range of 20-60kHz. After the L-H transition, the flux of this frequency range almost disappeared.

For the development of advanced fuelling method, compact toroid injection experiments were carried out. Rapid increase in line averaged density with time scale of 60  $\mu\text{s}$  was clearly

demonstrated.

### Acknowledgement

The authors appreciate Prof. K. Kawahata of National Institute for Fusion Science (NIFS) and Prof. S. Okajima of Chubu university for adjustment of FIR. They thank to Prof. K. Ida of NIFS for measurement of CXRS. They appreciate Dr. M. Azumi of JAERI for development of equilibrium code with ferritic steel. The authors are indebted to Dr. H. Kishimoto, Dr. S. Matsuda, Dr. A. Kitsunezaki, Dr. M. Shimizu, Dr. H. Ninomiya and Dr. M. Kikuchi of JAERI for their continuous encouragement and support.

### References

- [1] HISHINUMA, A., KOHYAMA, A., KLUEH, R.L., et al., J. Nucl. Mater. **258-263** (1998) 193.
- [2] SEKI, Y., KIKUCHI, M., ANDO, T., OHARA, Y., et al., Proc. Int. Conf. Plasma physics and controlled Nuclear Fusion Reserch (IAEA, Vienna 1990) Vol. 3,473.
- [3] IOKI, K., BARABASH, V., CARDELLA, A., et al., J. Nucl. Matter. **258-263** (1998) 74.
- [4] Turner, L. R., Wang, S. T., Stevens H. C., *Proc.3rd Topical Meeting on the Technology of Controlled Nuclear Fusion*, (Santa Fe, 1978) 883.
- [5] Sato, M., MIURA, Y. KIMURA,H. et al., J. Plasma Fusion Res. 75 (1999) 741.
- [6] HINO, T., HIROHATA, Y., YAMAUCHI, Y. et al., 18<sup>th</sup> IAEA Fusion Energy Conference, CN-77/FTP1/08 (Sorrento, 2000).
- [7] NAKAYAMA, T., ABE, M., TADOKORO T. et al., J. Nucl. Matter. **271&272** (1999) 491.
- [8] KAWASHIMA, H., SATO, M., TSUZUKI, K. et al., Nucl. Fusoin **41** (2001) 257.
- [9] NINOMIYA, H., KITSUNEZAKI, A., SHIMIZU,M. et al., Fusion Sci. Technol. **42** (2002) 7.
- [10] TSUZUKI, K., KIMURA, H., KAWASHIMA, H., et al, Proc. 10th Int. Conf. On Fusion Reactor Materials, J. Nucl. Mater. in press.
- [11] ISEI, N., SATO, M., TSUZUKI, K. et.al., Fusion Technol. **39** (2001) 1101.
- [12] La Haye, R. J., et al., Phys. Fluids **B4** (1992) 2098.
- [13] MORI, M. ET AL., Plasma Physics and Controlled Nuclear Fusion Reserch, Vol.2 IAEA (1992) 572.
- [14] ODAKA, K., SATO, O., OHTSUKA, M., et al., J. Plasma Fusion Res. 73 (1997) 1001(in Japanese).
- [15] TSUZUKI, K., SATO, M., KAWASHIMA, H., et al., Proc. 15th plasma surface interaction, to be published in J. Nucl. Mater.
- [16] SHINOHARA, K. ET AT., EX/P2-14 ,this conference.
- [17] JASSBY, D. L. and GOLDSTON, R. J., Nucl. Fusion **16** (1976) 613.
- [18] TANI, K., YOSHINO, R., TUDA, T., TAKIZUKA, T., and AZUMI, M., Fusion Tech. **21** (1992) 103.
- [19] HAMAMATSU, K et al., Plasma Phys. Control. Fusion **40** (1998) 255.
- [20] HOSHINO, K., NORI, M., YAMAMOTO T. et al., Phys. Rev Lett. 69 (1992) 2208.
- [21] YANAGISAWA, I., MORI, M., SHOJI, T. AND SUZUKI N., IEEE
- [22] SNIPES, J., ITER H-mode Threshold Database Working Group, 7th H-mode Workshop, Oxford, 1999; to be published in Plasma Phys. Control. Fusion.
- [23] KAMIYA, K. et al., EX/P2-5 this conference.
- [24] IDO, T., et al., Phys. Rev. Lett. **88** (2002).
- [25] FUKUMOTO, N. et al., FT/P2-07, this conference.